

# 1 The water balance components of undisturbed tropical 2 woodlands in the Brazilian Cerrado

3

4 P. T. S. Oliveira<sup>1,2,\*</sup>, E. Wendland<sup>1</sup>, M. A. Nearing<sup>2</sup>, R. L. Scott<sup>2</sup>, R. Rosolem<sup>3</sup>, and H. R. da  
5 Rocha<sup>4</sup>

6 <sup>1</sup>Department of Hydraulics and Sanitary Engineering, University of São Paulo, CxP. 359, São  
7 Carlos, SP, 13560-970, Brazil.

8 <sup>2</sup>USDA-ARS, Southwest Watershed Research Center, 2000 E. Allen Rd., Tucson, AZ 85719,  
9 United States.

10 <sup>3</sup>Queens School of Engineering, University of Bristol, Bristol, UK.

11 <sup>4</sup>Departamento de Ciências Atmosféricas, IAG, University of São Paulo, Sao Paulo, Brazil.

12 \*Correspondence to: P. T. S. Oliveira ([paulotarsoms@gmail.com](mailto:paulotarsoms@gmail.com))

13

14 **Abstract:** Deforestation of the Brazilian Cerrado region has caused major changes in  
15 hydrological processes. These changes in water balance components are still poorly  
16 understood, but are important for making land management decisions in this region. To better  
17 understand pre-deforestation conditions, we determined the main components of the water  
18 balance for an undisturbed tropical woodland classified as "cerrado sensu stricto denso". We  
19 developed an empirical model to estimate actual evapotranspiration (ET) by using flux tower  
20 measurements and, vegetation conditions inferred from the enhanced vegetation index and  
21 reference evapotranspiration. Canopy interception, throughfall, stemflow, surface runoff, and  
22 water table level were assessed from ground measurements. We used data from two Cerrado  
23 sites, "Pé de Gigante" - PDG and "Instituto Arruda Botelho" - IAB. Flux tower data from the  
24 PDG site collected from 2001 to 2003 were used to develop the empirical model to estimate  
25 ET. The other hydrological processes were measured at the field scale between 2011 and 2014  
26 in the IAB site. The empirical model showed significant agreement ( $R^2=0.73$ ) with observed  
27 ET at the daily time scale. The average values of estimated ET at the IAB site ranged from  
28 1.91 to 2.60 mm d<sup>-1</sup> for the dry and wet season, respectively. Canopy interception ranged  
29 from 4 to 20% and stemflow values were approximately 1% of gross precipitation. The

30 average runoff coefficient was less than 1%, while Cerrado deforestation has the potential to  
31 increase that amount up to 20 fold. As relatively little excess water runs off (either by surface  
32 water or groundwater) the water storage may be estimated by the difference between  
33 precipitation and evapotranspiration. Our results provide benchmark values of water balance  
34 dynamics in the undisturbed Cerrado that will be useful to evaluate past and future land cover  
35 and land use changes for this region.

36 **Keywords:** evapotranspiration, throughfall, stemflow, runoff, savanna, deforestation, water  
37 balance, canopy interception.

38

## 39 **1 Introduction**

40 As global demand for agricultural products such as food, fiber, and fuel grows to  
41 unprecedented levels, the supply of available land continues to decrease, which is acting as a  
42 major driver of cropland and pasture expansion across much of the developing world (Gibbs  
43 et al., 2010; Macedo et al., 2012). Vast areas of forest and savannas in Brazil have been  
44 converted into farmland, and there is little evidence that agricultural expansion will decrease,  
45 mainly because Brazil holds a great potential for further agricultural expansion in the twenty-  
46 first century (Lapola et al., 2014).

47 The Amazon rainforest and Brazilian savanna (Cerrado) are the most threatened biomes  
48 in Brazil (Marris, 2005). However, the high suitability of the Cerrado topography and soils for  
49 mechanized agriculture, the small number and total extent of protected areas, the lack of a  
50 deforestation monitoring program, and the pressure resulting from decreasing deforestation in  
51 Amazonia indicates that the Cerrado will continue to be the main region of farmland  
52 expansion in Brazil (Lapola et al., 2014). In fact, Soares-Filho et al. (2014) reported that the  
53 Cerrado is the most coveted biome for agribusiness expansion in Brazil, given its  $40 \pm 3$  Mha  
54 of land that could be legally deforested.

55 The Brazilian Cerrado, one of the richest ecoregions in the world in terms of the  
56 biodiversity (Myers et al., 2000), covers an area of 2 million km<sup>2</sup> (~22% of the total area of  
57 Brazil), however, areas of remaining native vegetation represent only 51% of this total  
58 (IBAMA/MMA/UNDP, 2011). In addition to being an important ecological and agricultural  
59 region for Brazil, the Cerrado is crucial to water resource dynamics of the country, and  
60 includes portions of 10 of Brazil's 12 hydrographic regions (Oliveira et al., 2014). Further, the

61 largest hydroelectric plants (comprising 80% of the Brazilian energy) are on rivers in the  
62 Cerrado. As savannas and forests have been associated with shifts in the location, intensity  
63 and timing of rainfall events, lengthening of the dry season and changed streamflow  
64 (Davidson et al., 2012; Spracklen et al., 2012; Wohl et al., 2012), it is clear that land cover  
65 and land use change promoted by the cropland and pasture expansion in this region have the  
66 potential to affect the ecosystems services and several important economic sectors of Brazil,  
67 such as agriculture, energy production and water supply.

68 Although all indications are that farmland expansion will continue in the Cerrado and  
69 that the land cover and land use will promote changes in water balance dynamics, few studies  
70 have been undertaken to investigate the hydrological processes at the field scale (plots or  
71 hillslope). In general, the studies on the Cerrado hydroclimatic variability have been done on  
72 large areas (Loraie et al., 2011; Davidson et al., 2012; Oliveira et al., 2014).  
73 Evapotranspiration (ET) has been the most intensively studied component of the water  
74 balance at the field scale, usually based on eddy covariance methods (Vourlitis et al., 2002;  
75 Santos et al., 2003; da Rocha et al., 2009; Giambelluca et al., 2009) or by the water balance in  
76 the soil (Oliveira et al., 2005; Garcia-Montiel et al., 2008). However, other water balance  
77 components such as rainfall interception, canopy throughfall, stemflow, surface runoff,  
78 infiltration, percolation, subsurface flow and groundwater recharge are poorly understood in  
79 the Cerrado due to lack of available observations.

80 To understand pre-deforestation conditions, the objective of this study was to determine  
81 the main components of the water balance for an undisturbed tropical woodland classified as  
82 "cerrado sensu stricto denso". We developed an empirical model to estimate actual  
83 evapotranspiration (ET) by using flux tower measurements and vegetation conditions inferred  
84 from the enhanced vegetation index (EVI) and reference crop evapotranspiration (ET<sub>o</sub>).  
85 Canopy interception, throughfall, stemflow, and surface runoff were assessed from ground  
86 measurements. We used data from two cerrado sites, "Pé de Gigante" - PDG and "Instituto  
87 Arruda Botelho" - IAB. Flux tower data from the PDG site collected from 2001 to 2003 was  
88 used to develop the empirical model to estimate ET. The other hydrological processes were  
89 measured at the field scale between 2011 and 2014 in the IAB site. A more comprehensive  
90 accounting of individual water balance components in the Brazilian Cerrado ecosystem is of  
91 paramount importance for understanding hydrological cycle shifts in the future due to  
92 possible land-use/land-cover changes.

93

## 94 **2 Data and Methods**

### 95 **2.1 Study Sites**

96 We developed this study using data from two cerrado sites, "Pé de Gigante" - PDG and  
97 "Instituto Arruda Botelho" - IAB, referenced throughout the text as PDG and IAB,  
98 respectively. Both sites are located in the State of São Paulo and are separated from each other  
99 by approximately 60 km (Fig. 1). The physiognomy of PDG and IAB sites was classified as  
100 "cerrado sensu stricto denso", which is also known as cerrado woodland, and has a  
101 characteristic arborous cover of 50% to 70% and trees with heights of 5 to 8 m (Furley 1999).  
102 Similar soil characteristics, hydroclimatology and phenology were found between these sites  
103 (Table 1).

104

105

*Insert Figure 1*

106

*Insert Table 1*

107

#### 108 ***'Pé de Gigante' site (PDG)***

109

110 We used field measurements collected at the PDG flux tower located on a contiguous  
111 1060 ha undisturbed woodland in the municipality of Santa Rita do Passo Quatro, São Paulo  
112 State (latitude 21°37' S, longitude 47°39' W, elevation:~ 700 m). According to the Köppen  
113 climate classification system, the climate in this area is Cwa humid subtropical, with a dry  
114 winter (April to September) and hot and rainy summer (October to March). The soil is  
115 classified in the Brazilian Soil Classification System (SiBCS) as Ortíc Quartzarénico Neosol  
116 (RQo) with less than 15% clay. Net radiation (R<sub>n</sub>), latent heat (LE), sensible heat (H) fluxes  
117 and ancillary meteorological data were measured at a height of 21 m and recorded every half-  
118 hour from January 2001 to December 2003. Details about the equipment and measurement  
119 procedures used are provided by da Rocha et al. (2002, 2009).

120

#### 121 ***'Instituto Arruda Botelho' site (IAB)***

122

123 The IAB site is a 300 ha, undisturbed woodland located in the municipality of Itirapina,  
124 São Paulo State (latitude 22°10' S, longitude 47°52' W, elevation: 780 m). The soil is also  
125 classified as Ortique Quartzarenic Neosol with sandy texture in the entire profile (85.7% sand,  
126 1.7% silt, and 12.6% clay), and soil bulk density of 1.7 g cm<sup>-3</sup>. We installed an 11 m  
127 instrumental platform to measure basic above-canopy meteorological and soil variables  
128 (Table 2). A datalogger (Campbell CR1000, Logan UT, USA) sampled the weather station  
129 and soil data every 15 s and recorded averages on a 10 min basis.

130

*Insert Table 2*

131

## 132 **2.2 Modeling Evapotranspiration**

133 In Brazil, there are a few flux tower sites in native cerrado vegetation. These sites were  
134 located in the States of São Paulo (da Rocha et al., 2002 and 2009), Brasília (Giambelluca et  
135 al., 2009; Miranda et al., 1997), and Mato Grosso (Vourlitis et al., 2002). There is a lack of  
136 information about ET in other Cerrado regions. To fill this gap, some authors have combined  
137 vegetation indices (VI) from the remote sensing data with ground measures of ET (usually  
138 flux tower) to spatially extrapolate ET measurements over nearby regions with few or no  
139 ground data. This process consists in the use of ground measurements of ET from flux towers  
140 set in natural ecosystems to develop a best-fit equation between ET, satellite-derived VIs,  
141 ancillary remote sensing data, and ground meteorological data (Glenn et al., 2010, 2011).  
142 Such an approach has been successfully applied to determine ET in natural ecosystems such  
143 as: riparian zones (Scott et al., 2008), shrublands (Nagler et al., 2007), rangeland and native  
144 prairie (Wang et al., 2007) temperate grassland, boreal forest, tundra (Mu et al., 2009) and  
145 Amazon rainforest (Joarez et al., 2008).

146 VIs are a ratio derived from the red and near-infrared spectral reflectance, and are  
147 strongly correlated with physiological processes that depend on photosynthetically active  
148 radiation absorbed by a canopy, such as transpiration and photosynthesis (Glenn et al., 2010).  
149 Normalized Difference Vegetation Index (NDVI) and the Enhanced Vegetation Index (EVI)  
150 from the Moderate Resolution Imaging Spectrometer (MODIS) on the NASA Terra satellite  
151 are VIs widely used in environmental studies. However, previous studies have shown that  
152 EVI can better capture canopy structural variation, seasonal vegetation variation, land cover

153 variation, and biophysical variation for high biomass vegetation (Huete et al. 2002; Joarez et  
154 al., 2008). In addition, EVI has been a better predictor of ET than NDVI (Nagler et al., 2005a,  
155 b; Glenn et al., 2007; Wang et al., 2007).

156 We developed an empirical relationship between ET from the PDG flux tower, MODIS  
157 Enhanced Vegetation Index (EVI) and reference crop evapotranspiration (ET<sub>o</sub>) following the  
158 approach used by Nagler et al. (2013):

$$159 \quad ET = ET_o [ a (1 - e^{(-bEVI)}) - c ] \quad (1)$$

160 where  $a$ ,  $b$  and  $c$  are fitting coefficients and  $(1 - e^{(-bEVI)})$  is derived from the Beer-Lambert  
161 Law modified to predict absorption of light by a canopy. The coefficient  $c$  accounts for the  
162 fact that EVI is not zero at zero ET since bare soil has a low but positive EVI (Nagler et al.,  
163 2004, 2013).

164 Daily average ET values from the PDG flux tower were computed by first filling the  
165 gaps in the 1-hour data that were due to sensor malfunctions or bad measurements. Gaps were  
166 filled using 1-hour averages of photosynthetically active radiation (PAR) and a 14-day look-  
167 up tables of ET values averaged over 100 micromoles  $m^{-2} s^{-1}$  intervals (Falge et al., 2001).  
168 Then we computed daily ET averages over every 16 days to be in sync with the 16-day EVI  
169 data. We used EVI data provided by the MODIS product MOD13Q1 (  
170 <http://daac.ornl.gov/MODIS/>). These data are provided by National Aeronautics and Space  
171 Administration (NASA) as atmospherically and radiometrically corrected 16-day composite  
172 images with a 250 m spatial resolution. We obtained the MODIS EVI pixel centered on the  
173 flux tower. Daily ET<sub>o</sub> was computed according to the FAO-56 method (Allen et al., 1998)  
174 and then averaged over 16 days.

175 We used the parameter optimization tool Genetic Algorithm to fit Eq. 1, incorporating  
176 the time series of measured ET, EVI and ET<sub>o</sub> for 2001 through 2003. This process consisted  
177 of minimizing the sum of squared differences between the ET observed from eddy covariance  
178 and estimated by Eq. 1:

$$179 \quad function = \sum_{i=1}^n [ET(i)obs - ET(i)sim]^2 \quad (2)$$

180 where  $ET(i)obs$  is the observed ET and  $ET(i)sim$  is modeled ET at time (i).

181 For model validation, we calibrated the model using 2001 and 2002 data and then  
182 predicted ET for 2003. After this validation process we fit Eq. 1 again, but this time  
183 considering the full time series that was available. The coefficient of determination ( $R^2$ ),

184 standard deviation of differences between observed and estimated ET (*SD*), root mean square  
185 (*RMSE*) and the Student's t-test with a 95% confidence level were used to evaluate the  
186 significance of the linear relationship between the observed and estimated ET.

187

## 188 **2.3 Hydrological processes measured at the IAB site**

### 189 ***Canopy interception***

190 Canopy interception (CI) was computed as the difference between the gross  
191 precipitation ( $P_g$ ) and the net precipitation ( $P_n$ ), where  $P_g$  is the total precipitation that fell at  
192 the top of the canopy and  $P_n$  was computed as the sum of two components: throughfall (TF)  
193 and stemflow (SF):

$$194 \quad CI = P_g - P_n = P_g - (TF + SF) \quad (3)$$

195 We measured the  $P_g$  from an automated tipping bucket rain gauge (model TB4) located  
196 above the canopy at 11 m height (Table 2). TF was obtained from 15 automated tipping  
197 bucket rain gauges (Davis Instruments, Hayward, CA) distributed below the cerrado canopy  
198 and randomly relocated every month during the wet season. Each rain gauge was installed  
199 considering an influence area of 10 x 10 m. SF was measured on 12 trees using a plastic hose  
200 wrapped around the trees trunks, sealed with neutral silicone sealant, and a covered bucket to  
201 store the water. Selected trees to be monitored were divided into two groups considering the  
202 diameter at breast height (DBH), which is the tree diameter measured at 1.30 m above the  
203 ground. Therefore, we monitored 7 trees with  $5 \text{ cm} < \text{DBH} < 20 \text{ cm}$  and 5 trees with  $\text{DBH} >$   
204  $20 \text{ cm}$ . The volume of water in each SF collector was measured after each rainfall event that  
205 generated stemflow, totaling 42 SF measurements during the study period. The volume of  
206 water measured from each sample tree was expressed as an equivalent volume per  $\text{m}^2$  of basal  
207 area, and then this value was multiplied by the site basal area ( $27.75 \text{ m}^2 \text{ ha}^{-1}$ ) to compute  
208 stemflow in mm (Dezseo and Chacón, 2006 and MacJannet et al., 2007). We measured  $P_g$ , TF  
209 and SF from September 2012 to July 2014.

210

### 211 ***Surface runoff***

212 Surface runoff was measured from  $100 \text{ m}^2$  experimental plots of 5 m width and 20 m  
213 length from January 2012 to July 2014. To evaluate the cover influence on the surface runoff,

214 experimental plots were installed under native vegetation and bare soil with steepness of  
215 approximately  $0.09 \text{ m m}^{-1}$ . Each treatment had three replications and plots on bare soil were  
216 located about 1 km from the plots under undisturbed cerrado. The boundaries of the plots  
217 were made using galvanized sheet placed 30 cm above the soil and into the soil to a depth of  
218 30 cm. Surface runoff was collected in storage tanks at the end of each plot. Plots under bare  
219 soil were built with three storage tanks with 310 liters capacity each and two splitters of one  
220 seventh, i.e. one seventh were collected in the second tank and one forty ninth in the third  
221 tank. In the plots under cerrado vegetation only one storage tank with a capacity of 310 liters  
222 for each plot was used to collect runoff and soil loss because of the expected lower runoff  
223 amounts from those plots.

224 Surface runoff was measured for each erosive rain event under the undisturbed cerrado  
225 and bare soil. Periods of rainfall were considered to be isolated events when they were  
226 separated by periods of precipitation between 0 (no rain) and 1.0 mm for at least 6 h, and were  
227 classified as erosive events when 6.0 mm of rain fell within 15 min or 10.0 mm of rain fell  
228 over a longer time period (Oliveira et al., 2013). We used this approach because in general  
229 only erosive rainfall has promoted surface runoff in the study area. A total of 65 erosive  
230 rainfall events were evaluated during the study period.

### 231 ***Groundwater recharge***

232 The water table level was monitored from December 2011 to July 2014 from a well  
233 with 42 m in depth installed in the undisturbed Cerrado. Water-table fluctuation data were  
234 measured daily from a pressure sensor (Mini-Diver model DI501, Schlumberger Limited,  
235 Houston, USA).

236

## 237 **2.4 Water balance at the IAB site**

238 We evaluated the water balance components in the IAB site at the daily, monthly and  
239 annual time scales from January 2012 to March 2014 (Eq. 4). We used measured data of  
240 precipitation, surface runoff, and direct recharge. Evapotranspiration was estimated using the  
241 fitted equation from the EVI and reference evapotranspiration data.

$$242 \quad \frac{dS}{dt} = P - ET - Q - R \quad (4)$$



243 where  $S$  is the soil water storage change with time,  $P$  is precipitation,  $ET$  is  
244 evapotranspiration,  $Q$  is runoff, and  $R$  groundwater recharge.

245

### 246 **3 Results and Discussion**

#### 247 **3.1 Modeling ET**

248 The daily average ( $\pm$  standard deviation) reference evapotranspiration ( $ET_o$ ), measured  
249 evapotranspiration ( $ET$ ), and EVI at the PDG site were  $4.56 \pm 0.73 \text{ mm d}^{-1}$ ,  $2.31 \pm 0.87 \text{ mm d}^{-1}$ ,  
250  $1$ , and  $0.41 \pm 0.09$ , respectively. We found a significant correlation between observed  $ET$  and  
251  $EVI$  with a correlation coefficient of  $0.75$  ( $p < 0.0001$ ).  $EVI$  showed similar seasonality that  
252 was observed for the  $ET$  and  $ET_o$  during wet and dry seasons (Fig. 2). The average  $ET$  and  
253  $EVI$  values for the wet season were  $2.81 \pm 0.57 \text{ mm d}^{-1}$  and  $0.48 \pm 0.05$ , and for the dry  
254 season  $1.70 \pm 0.70 \text{ mm d}^{-1}$  and  $0.33 \pm 0.05$ , respectively.

255

256

257

*Insert Figure 2*

258

259 The fitted equation considering the periods of calibration, validation and full time series  
260 at 16-day averages showed good results in the  $ET$  estimates, with a coefficient of  
261 determination ( $R^2$ ) greater than  $0.70$  and standard deviation of differences between observed  
262 and estimated  $ET$  ( $SD$ ) and root mean square ( $RMSE$ ) less than  $0.50 \text{ mm d}^{-1}$  and  $21\%$ ,  
263 respectively (Table 3). The final form of the fitted equation was:

$$264 \quad ET = ET_o [ 10.36 (1 - e^{(-12.31EVI)}) - 9.74 ] \quad (5)$$

265

266

*Insert Table 3*

267

268 The modeled values of  $ET$  estimated for the full period, wet and dry seasons ( $2.30 \pm$   
269  $0.76 \text{ mm d}^{-1}$ ,  $2.81 \pm 0.31 \text{ mm d}^{-1}$ , and  $1.69 \pm 0.60 \text{ mm d}^{-1}$ , respectively) were not significantly  
270 different ( $p = 0.05$ ) from the observed values of  $ET$  during the same period. Furthermore, we  
271 found better values of  $R^2$ ,  $SD$ , and  $RMSE$  of  $0.78$ ,  $0.16 \text{ mm month}^{-1}$ , and  $17.07\%$  at the

272 monthly scale. The annual average ET observed and estimated for the three years studied  
273 (2001-2003) were 822 mm yr<sup>-1</sup> and 820 mm yr<sup>-1</sup>, respectively, with an RMSE of 6.12%.  
274 Observed ET during 2001 from the PDG site was compared previously by Ruhoff et al.  
275 (2013) with the ET estimated from the product MOD16 (Mu et al., 2011). The authors found  
276 values of  $R^2 = 0.61$  and  $RMSE = 0.46 \text{ mm d}^{-1}$ , which were not as good as for the present study  
277 results. In a review paper about ET estimation in natural ecosystems using vegetation index  
278 methods, Glenn et al. (2010) reported values for different temporal scales ranging from 0.45  
279 to 0.95 for the  $R^2$  and of 10 to 30% for the RMSE. They concluded that the uncertainty  
280 associated with remote sensing estimates of ET is constrained by the accuracy of the ground  
281 measurements, which for the flux tower data are on the order of 10 to 30%. Hence, the values  
282 of SD and RMSE reported in the present study are within the error bounds of the likely  
283 ground measurement errors. Our findings indicate that from this fitted equation is possible to  
284 compute ET at 16 days and these results may be interpolated and/or summed to estimate  
285 daily, monthly or annual values.

286

### 287 **3.2 Canopy interception, throughfall, and stemflow**

288 The gross precipitation ( $P_g$ ) in the IAB site during the 23 month study period was 1929  
289 mm, where 78% of this total occurred from October through March (wet season). We found  
290 similar values of 766 mm and 734 mm for the two wet seasons studied, 2012-2013 and 2013-  
291 2014. We found a total of 333 mm in the dry season of 2013 (which is similar to the historical  
292 mean in this season of 307 mm) and 92 mm between the months April through July of 2014  
293 (Fig. 3a). The sum of throughfall (TF) was 1566 mm, which corresponded to 81.2% of  $P_g$ .  
294 Individual wet season TF values were 81.9 and 82.3% of  $P_g$  while total dry season  $P_g$  was  
295 74.8%. The coefficient of determination between  $P_g$  and TF was 0.99 ( $p < 0.0001$ ) over the  
296 253 rainfall days (Fig. 3b). Stemflow values (by 42 events) ranged from 0.3 to 2.7% with an  
297 average of 1.1% of  $P_g$ . The greatest values of SF were found in the beginning of the wet  
298 season (October and November) and the smallest values occurred in the middle of the wet  
299 season (January and February). This suggests that there is an influence of condition of trees  
300 trunks (dry and wet) and canopy dynamics in the stemflow. Furthermore, we found greater  
301 values of SF in the trees with  $5 \text{ cm} < \text{DBH} < 20 \text{ cm}$  (1.6% of  $P_g$ ) than the trees with  $\text{DBH} >$   
302  $20 \text{ cm}$  (0.4% of  $P_g$ ), which is consistent with results reported by Bäse et al. (2012) for the  
303 transitional Amazonia–Cerrado forest.

304

305

*Insert Figure 3*

306

307 We found only three previous studies about interception process in the Brazilian  
308 Cerrado. The values reported in the literature for TF and SF, ranged from 80 to 95% of  $P_g$ .  
309 and <1 to 2.4% of  $P_g$ , respectively (Table 4). In the present study the canopy interception (CI)  
310 was 17.7% of  $P_g$ . Therefore, considering our findings and previous studies presented in Table  
311 4 we can suggest that CI in the undisturbed cerrado ranges from 4 to 20% of  $P_g$ . However,  
312 future studies are necessary to understand the influence of physiognomies of the Cerrado in  
313 the CI processes. This region is large and complex and varies from grassland to savanna to  
314 forest (Furley, 1999; Ferreira and Huete, 2004). In addition, other characteristics such as  
315 conditions trees trunks (crooked and twisted), stand structure, canopy cover, rainfall features,  
316 and the litter interception should be better studied in specific studies of rainfall interception  
317 processes.

318

319

*Insert Table 4*

320

### 321 **3.3 Cerrado water balance**

322 The measured annual precipitation at the IAB site was 1248 mm, 1139 mm, 421 mm for  
323 2012, 2013 and January through July of 2014, respectively. We measured 65 rainfall events  
324 that generated surface runoff during the study. The runoff coefficient for individual rainfall  
325 events (total runoff divided by total rainfall) ranged from 0.003 to 0.860 with an average  
326 value and standard deviation of  $0.197 \pm 0.179$  in the bare soil plots. The highest values were  
327 found for larger, more intense rainfall events, or in periods with several consecutive rainfall  
328 events, which induced high soil moisture contents and consequently greater runoff generation.  
329 Moreover, the runoff coefficient found for the bare soil plots (~20%) indicates that the soil in  
330 the study area (sandy soil) has a high infiltration capacity. Runoff coefficients ranged from  
331 0.001 to 0.030 with an average of less than 1% ( $0.005 \pm 0.005$ ) in the plots under undisturbed  
332 cerrado. Youlton (2013) studied in two hydrological years (2011-12 and 2012-13) the surface  
333 runoff using plots installed in the same experimental area as the present study and found  
334 values of 3.6 to 5.1% and 2.0 to 5.0% for the runoff coefficient under pasture and sugarcane,

335 respectively. Cogo et al. (2003) reported values of runoff coefficient for soybeans and oat  
336 ranging from 2.0 to 4.0% depending to the soil tillage and management. Pasture, sugarcane  
337 and soybeans are the main cover types that have been used to replace the undisturbed cerrado  
338 lands (Loarie et al., 2011; Lapola et al., 2014). Therefore our results indicate that the cerrado  
339 deforestation has the potential to increase surface runoff around 5 fold when the cerrado is  
340 replaced for pasture and croplands and up to 20 fold for bare soil conditions.

341 Infiltration was calculated after subtracting interception (without accounting for the  
342 litter interception) and surface runoff from the gross precipitation. Thereby we found that  
343 79% of gross rainfall infiltrated into the soil. Fig. 4 shows the amount of infiltration and the  
344 volumetric water content (VWC) up to 1.5 m in depth. We found a rapid increase in the VWC  
345 as a function of infiltration, indicating that the sandy soil found in the IAB site promoted fast  
346 infiltration, mainly in the first meter depth of the soil profile. VWC ranged from 0.08 to 0.23  
347  $\text{m}^3 \text{m}^{-3}$  and 0.08 to 0.17  $\text{m}^3 \text{m}^{-3}$  for 0.1 and 1.5 m soil depths, respectively. However, it is  
348 important to note that the root zone for trees in the cerrado is usually deep (more than 10 m in  
349 depth) and limited by the water table level (Oliveira et al, 2005; Garcia-Montiel et al., 2008;  
350 Villalobos-Vega et al., 2014). Therefore, the 1.5 m soil profile is not representative for  
351 evaluating the water use by vegetation, but is useful to evaluate the response for rainfall  
352 events and evaporative processes. Oliveira et al. (2005) concluded that the water stored in  
353 deep soil layers (1 to 4 m) provides approximately 75% of the total water used for an  
354 undisturbed cerrado classified as "cerrado sensu stricto denso", the class that includes the IAB  
355 and PDG sites.

356

357

*Insert Figure 4*

358

359 The amount of water infiltrated into the soil was not enough to elevate the water table  
360 level in the well during the study period, from December 2011 to July 2014. This was because  
361 the water table in the monitored well was approximately 35 m deep. In other words, there is a  
362 large distance from the soil surface to the water tables, and the amount of water that  
363 eventually reached the saturated zone was not enough to cause an immediate change in the  
364 water table level. One of the first studies of groundwater dynamics in the undisturbed cerrado  
365 was conducted by Villalobos-Vega et al., (2014) from 11 monitored wells with water tables  
366 ranging from 0.18 to 15.56 m. The authors found little water table change in regions with

367 deep water table (up to 15.56 m), and in some wells the recharge water took up to 5 months to  
368 reach the groundwater table. They also concluded that water table depth has a strong influence  
369 on variations in tree density and diversity, i.e. regions with deep water tables such as the IAB  
370 site (35 m) tend to exhibit greater tree abundance and diversity than sites with shallow water  
371 table. Therefore, the infiltrated water in the present study was likely either extracted and  
372 transpired by the vegetation, drained by lateral subsurface flow (not measured in this studied,  
373 but probably small due to the flat topography of the site) or stored in the vadose zone.

374 Groundwater recharge is also affected by land use and land cover change (Scanlon et  
375 al., 2005; Dawes et al., 2012). We found that the undisturbed cerrado tends to provide more  
376 infiltration than areas covered with pasture and cropland. On the other hand, the cerrado  
377 vegetation has significant canopy interception and evapotranspiration that result in little  
378 groundwater recharge as compared to pasture and cropland. Using 23 monitoring wells  
379 distributed in a watershed located 5 km away from the IAB site, Wendland et al. (2007)  
380 showed that the groundwater recharge varies with the land cover. The authors reported values  
381 of annual recharge and water table depth, respectively, ranging from 145 to 703 mm yr<sup>-1</sup> (5  
382 to 16 m) in pasture, 324–694 mm yr<sup>-1</sup> (9 to 22 m) in orange citrus, and 37–48 mm yr<sup>-1</sup> (21 m)  
383 in eucalyptus forests. Therefore, cerrado deforestation has the potential to change  
384 groundwater recharge dynamics.

385 The average values of actual evapotranspiration (ET) estimated by Eq. 5 for the IAB  
386 Cerrado site for the full period, wet and dry seasons were similar to that observed in the PDG  
387 site (Table 5). The annual average ET estimated for the two years studied (2012-2013) was  
388 823 mm yr<sup>-1</sup>, which also is consistent with that found by Giambelluca et al. (2009) of 823 mm  
389 yr<sup>-1</sup> and the PDG site of 822 mm yr<sup>-1</sup>. Given that surface runoff was less than 1% of  
390 precipitation and groundwater recharge and subsurface lateral flow was likely small, vadose  
391 zone water storage is basically the difference between precipitation and evapotranspiration  
392 (Fig. 5).

393

394

*Insert Table 5*

395

*Insert Figure 5*

396

397 Water deficits in the Cerrado region usually happen from April through September (dry  
398 season), however we found an atypical water decrease in the wet season (months of March  
399 and November 2012, and January 2014). Indeed, the rainfall amounts in these months were  
400 71%, 56% and 39% less than the historical mean of 1973 to 2013 (156 mm, 147 mm and 270  
401 mm) observed at the climatological station from the Centro de Recursos Hídricos e Ecologia  
402 Aplicada at the University of São Paulo, located approximately 3 km from the study area. In  
403 addition, we note that the annual rainfall during the period of study (1248 mm and 1139 mm  
404 for 2012 and 2013, respectively) were approximately 20% less than the historical mean of the  
405 1500 mm. The decreased rainfall in São Paulo State in recent years has caused problems of  
406 water scarcity (Rodrigues et al., 2014).

407

#### 408 **4 Conclusions**

409 We developed an empirical model to estimate actual evapotranspiration by using flux  
410 tower measurements and, vegetation conditions inferred from the enhanced vegetation index  
411 and reference evapotranspiration. We used flux tower data from the PDG site collected during  
412 2001 to 2003. The empirical model developed in the present study showed a significant  
413 agreement with observed ET and better results than from the product MOD16 ET. From this  
414 empirical model is possible to compute ET at 16 days and these results may be interpolated  
415 and/or summed to estimate daily, monthly or annual values for undisturbed cerrado areas with  
416 similar characteristics of hydroclimatology and phenology that observed at the PDG site.  
417 Furthermore, from this approach it is possible to assess the ET for large areas of the Cerrado  
418 with a good spatial and temporal resolution (250 m and 16 days), therefore, it may be useful  
419 for monitoring evapotranspiration dynamics in this region.

420 Canopy interception, throughfall, stemflow, surface runoff, and water table level were  
421 assessed from ground-measurements at the field scale between 2011 and 2014 at the IAB site.  
422 We conclude that the canopy interception may range from 4 to 20% of gross precipitation in  
423 the cerrado and that stemflow values are around 1% of gross precipitation. Our results also  
424 indicate that the average runoff coefficient was less than 1% in the plots under undisturbed  
425 cerrado and that the deforestation has the potential to increase up to 20 fold the runoff  
426 coefficient value. In addition, we did not find evidence of net groundwater table changes,  
427 possibly because the water table is at significant depth at the IAB site, the deep rooting depth  
428 of the trees, and the study period with rainfall smaller than the historical mean. As only little

429 excess water runs off (either by surface water or groundwater) the water storage may be  
430 estimated by the difference between precipitation and evapotranspiration.

431 Deforestation of the Brazilian Cerrado has caused major changes in hydrological  
432 processes; however these changes are still poorly understood at the field scale. Thus,  
433 understanding pre-deforestation conditions including the main components of the water  
434 balance is of paramount importance for an undisturbed cerrado. In this study, we provide  
435 benchmark values of water balance dynamics in the undisturbed Cerrado that will be useful to  
436 evaluate past and future land use in different sceneries of water scarcity and climate change  
437 for this region.

438

### 439 **Acknowledgments**

440 This study was supported by grants from the Fundação de Amparo à Pesquisa do  
441 Estado de São Paulo - FAPESP (10/18788-5, 11/14273-3 and 12/03764-9) and the Conselho  
442 Nacional de Desenvolvimento Científico e Tecnológico - CNPq (470846/2011-9). USDA is  
443 an equal opportunity provider and employer. We would like to thank the Arruda Botelho  
444 Institute (IAB) and São José farm that have allowed us to develop this study in the native  
445 Cerrado vegetation. Finally, we appreciate valuable comments and careful reviews from  
446 editors, and the anonymous reviewers who helped significantly to improve this manuscript.

447

### 448 **References**

449 Allen, R., L. Pereira, D. Raes, M. Smith, K. Solomon, and T. O'Halloran, (1998), Crop  
450 Evapotranspiration-Guidelines for Computing Crop Water Requirements; FAO Irrigation  
451 and Drainage Paper 56; Food and Agriculture Organization of the United Nations: Rome,  
452 Italy.

453 Bäse, F., Elsenbeer, H., Neill, C. and Krusche, A. V.: Differences in throughfall and net  
454 precipitation between soybean and transitional tropical forest in the southern Amazon,  
455 Brazil, *Agr. Ecosyst. Environ.*, 159, 19–28, doi:10.1016/j.agee.2012.06.013, 2012.

456 Cogo, N. P., Levien, R. and Schwarz, R. A.: Perdas de solo e água por erosão hídrica  
457 influenciadas por métodos de preparo, classes de declive e níveis de fertilidade do solo, *R.*  
458 *Bras. Ci. Solo*, 27(4), 743–753, doi:10.1590/S0100-06832003000400019, 2003.

459 da Rocha, H. R. da, Freitas, H. C., Rosolem, R., Juárez, R. I. N., Tannus, R. N., Ligo, M. A.,  
460 Cabral, O. M. R. and Dias, M. A. F. S.: Measurements of CO<sub>2</sub> exchange over a woodland  
461 savanna (Cerrado *Sensu stricto*) in southeast Brasil, *Biota neotrop.*, 2(1), 1–11,  
462 doi:10.1590/S1676-06032002000100009, 2002.

463 da Rocha, H. R., Manzi, A. O., Cabral, O. M., Miller, S. D., Goulden, M. L., Saleska, S. R.,  
464 Coupe, N. R., Wofsy, S. C., Borma, L. S., Artaxo, P., Vourlitis, G., Nogueira, J. S.,  
465 Cardoso, F. L., Nobre, A. D., Kruijt, B., Freitas, H. C., von Randow, C., Aguiar, R. G., and  
466 Maia, J. F.: Patterns of water and heat flux across a biome gradient from tropical forest to  
467 savanna in Brazil, *J. Geophys. Res.*, 114, 1-8, doi:10.1029/2007JG000640, 2009.

468 Davidson, E. A., de Araújo, A. C., Artaxo, P., Balch, J. K., Brown, I. F., Bustamante, M. M.  
469 C, Coe, M. T., DeFries, R. S., Keller, M., Longo, M., Munger, J. W., Schroeder, W.,  
470 Soares-Filho, B. S., Souza, C. M., and Wofsy, S. C.: The Amazon basin in transition,  
471 *Nature*, 481, 321–328, doi:10.1038/nature10717, 2012.

472 Dawes, W., Ali, R., Varma, S., Emelyanova, I., Hodgson, G. and McFarlane, D.: Modelling  
473 the effects of climate and land cover change on groundwater recharge in south-west  
474 Western Australia, *Hydrol. Earth Syst. Sci.*, 16(8), 2709–2722, doi:10.5194/hess-16-2709-  
475 2012, 2012.

476 Dezzeo, N. and Chacón, N.: Nutrient fluxes in incident rainfall, throughfall, and stemflow in  
477 adjacent primary and secondary forests of the Gran Sabana, southern Venezuela, *For. Ecol.*  
478 *Manage.*, 234(1-3), 218–226, doi:10.1016/j.foreco.2006.07.003, 2006.

479 Falge, E., Baldocchi, D., Olson, R., Anthoni, P., Aubinet, M., Bernhofer, C., Burba, G.,  
480 Ceulemans, R., Clement, R., Dolman, H., Granier, A., Gross, P., Grünwald, T., Hollinger,  
481 D., Jensen, N.-O., Katul, G., Keronen, P., Kowalski, A., Ta Lai, C., Law, B. E., Meyers,  
482 T., Moncrieff, J., Moors, E., William Munger, J., Pilegaard, K., Rannik, Ü., Rebmann, C.,  
483 Suyker, A., Tenhunen, J., Tu, K., Verma, S., Vesala, T., Wilson, K. and Wofsy, S.: Gap  
484 filling strategies for long term energy flux data sets, *Agric. For. Meteorol.*, 107(1), 71–77,  
485 doi:10.1016/S0168-1923(00)00235-5, 2001.

486 Ferreira, L. G. and Huete, A. R.: Assessing the seasonal dynamics of the Brazilian Cerrado  
487 vegetation through the use of spectral vegetation indices, *Int. J. Remote Sens.*, 25(10),  
488 1837–1860, doi:10.1080/0143116031000101530, 2004.



489 Fidelis, A. T. and Godoy, S. A. P. de: Estrutura de um cerrado strico sensu na Gleba Cerrado  
490 Pé-de-Gigante, Santa Rita do Passa Quatro, SP, *Acta Bot. Bras.*, 17(4), 531–539,  
491 doi:10.1590/S0102-33062003000400006, 2003.

492 Furley, P. A.: The nature and diversity of neotropical savanna vegetation with particular  
493 reference to the Brazilian cerrados, *Global Ecol. Biogeogr.*, 8(3-4), 223–241,  
494 doi:10.1046/j.1466-822X.1999.00142.x, 1999.

495 Garcia-Montiel, D. C., Coe, M. T., Cruz, M. P., Ferreira, J. N., da Silva, E. M. and Davidson,  
496 E. A.: Estimating Seasonal Changes in Volumetric Soil Water Content at Landscape Scales  
497 in a Savanna Ecosystem Using Two-Dimensional Resistivity Profiling, *Earth Interact.*,  
498 12(2), 1–25, doi:10.1175/2007EI238.1, 2008.

499 Giambelluca, T. W., Scholz, F. G., Bucci, S. J., Meinzer, F. C., Goldstein, G., Hoffmann, W.  
500 A., Franco, A. C. and Buchert, M. P.: Evapotranspiration and energy balance of Brazilian  
501 savannas with contrasting tree density, *Agric. For. Meteorol.*, 149(8), 1365–1376,  
502 doi:10.1016/j.agrformet.2009.03.006, 2009.

503 Gibbs, H. K., Ruesch, A. S., Achard, F., Clayton, M. K., Holmgren, P., Ramankutty, N. and  
504 Foley, J. A.: Tropical forests were the primary sources of new agricultural land in the  
505 1980s and 1990s, *P. Natl. Acad. Sci. USA*, 107(38), 16732–16737,  
506 doi:10.1073/pnas.0910275107, 2010.

507 Glenn, E. P., Huete, A. R., Nagler, P. L., Hirschboeck, K. K. and Brown, P.: Integrating  
508 Remote Sensing and Ground Methods to Estimate Evapotranspiration, *Crit. Rev. Plant*  
509 *Sci.*, 26(3), 139–168, doi:10.1080/07352680701402503, 2007.

510 Glenn, E. P., Nagler, P. L. and Huete, A. R.: Vegetation Index Methods for Estimating  
511 Evapotranspiration by Remote Sensing, *Surv. Geophys.*, 31(6), 531–555,  
512 doi:10.1007/s10712-010-9102-2, 2010.

513 Glenn, E. P., Neale, C. M. U., Hunsaker, D. J. and Nagler, P. L.: Vegetation index-based crop  
514 coefficients to estimate evapotranspiration by remote sensing in agricultural and natural  
515 ecosystems, *Hydrol. Process.*, 25(26), 4050–4062, doi:10.1002/hyp.8392, 2011.

516 Honda, E. A.: Repartição da água da chuva sob o dossel e umidade do solo no gradiente  
517 fisionômico da vegetação do Cerrado, Ph.D. Thesis , Universidade de São Paulo, São  
518 Carlos, SP, Brazil, 2013.

519 Huete, A., Didan, K., Miura, T., Rodriguez, E. P., Gao, X. and Ferreira, L. G.: Overview of  
520 the radiometric and biophysical performance of the MODIS vegetation indices, *Remote*  
521 *Sens. Environ.*, 83(1–2), 195–213, doi:10.1016/S0034-4257(02)00096-2, 2002.

522 IBAMA/MMA/UNDP: Monitoramento do desmatamento nos biomas Brasileiros por satélite,  
523 Ministério de Meio Ambiente, Brasília, Brazil, available at:  
524 <http://siscom.ibama.gov.br/monitorabiomas/cerrado/index.htm> (last access: 1 September  
525 2014), 2011.

526 Lapola, D. M., Martinelli, L. A., Peres, C. A., Ometto, J. P. H. B., Ferreira, M. E., Nobre, C.  
527 A., Aguiar, A. P. D., Bustamante, M. M. C., Cardoso, M. F., Costa, M. H., Joly, C. A.,  
528 Leite, C. C., Moutinho, P., Sampaio, G., Strassburg, B. B. N. and Vieira, I. C. G.:  
529 Pervasive transition of the Brazilian land-use system, *Nature Climate Change*, 4(1), 27–35,  
530 doi:10.1038/nclimate2056, 2013.

531 Lilienfein, J. and Wilcke, W.: Water and element input into native, agri- and silvicultural  
532 ecosystems of the Brazilian savanna, *Biogeochemistry*, 67(2), 183–212,  
533 doi:10.1023/B:BIOG.0000015279.48813.9d, 2004.

534 Lima, W. P. and Nicolielo N.: Precipitação efetiva e interceptação em florestas de pinheiros  
535 tropicais e em reserva de cerrado. *IPEF*, 24, 43-46, 1983.

536 Loarie, S. R., Lobell, D. B., Asner, G. P., Mu, Q. and Field, C. B.: Direct impacts on local  
537 climate of sugar-cane expansion in Brazil, *Nature Climate Change*, 1(2), 105–109,  
538 doi:10.1038/nclimate1067, 2011.

539 Macedo, M. N., DeFries, R. S., Morton, D. C., Stickler, C. M., Galford, G. L. and  
540 Shimabukuro, Y. E.: Decoupling of deforestation and soy production in the southern  
541 Amazon during the late 2000s, *P. Natl. Acad. Sci. USA*, 109(4), 1341–1346,  
542 doi:10.1073/pnas.1111374109, 2012.

543 Marris, E.: Conservation in Brazil: The forgotten ecosystem, *Nature*, 437(7061), 944–945,  
544 doi:10.1038/437944a, 2005.

545 McJannet, D., Wallace, J. and Reddell, P.: Precipitation interception in Australian tropical  
546 rainforests: I. Measurement of stemflow, throughfall and cloud interception, *Hydrol.*  
547 *Process.*, 21(13), 1692–1702, doi:10.1002/hyp.6347, 2007.

548 Miranda, A. C., Miranda, H. S., Lloyd, J., Grace, J., Francey, R. J., McIntyre, J. A., Meir, P.,  
549 Riggan, P., Lockwood, R. and Brass, J.: Fluxes of carbon, water and energy over Brazilian  
550 cerrado: an analysis using eddy covariance and stable isotopes, *Plant. Cell Environ.*, 20(3),  
551 315–328, n.d.

552 Mu, Q., Jones, L. A., Kimball, J. S., McDonald, K. C., and Running, S. W.: Satellite  
553 assessment of land surface evapotranspiration for the pan-Arctic domain, *Water Resour.*  
554 *Res.*, 45, 1-20, doi:10.1029/2008WR007189, 2009.

555 Mu, Q., Zhao, M. and Running, S. W.: Improvements to a MODIS global terrestrial  
556 evapotranspiration algorithm, *Remote Sens. Environ.*, 115(8), 1781–1800,  
557 doi:10.1016/j.rse.2011.02.019, 2011.

558 Myers, N., Mittermeier, R. A., Mittermeier, C. G., da Fonseca, G. A. B. and Kent, J.:  
559 Biodiversity hotspots for conservation priorities, *Nature*, 403(6772), 853–858,  
560 doi:10.1038/35002501, 2000.

561 Nagler, P. L., Cleverly, J., Glenn, E., Lampkin, D., Huete, A. and Wan, Z.: Predicting riparian  
562 evapotranspiration from MODIS vegetation indices and meteorological data, *Remote Sens.*  
563 *Environ.*, 94(1), 17–30, doi:10.1016/j.rse.2004.08.009, 2005b.

564 Nagler, P. L., Glenn, E. P., Kim, H., Emmerich, W., Scott, R. L., Huxman, T. E. and Huete,  
565 A. R.: Relationship between evapotranspiration and precipitation pulses in a semiarid  
566 rangeland estimated by moisture flux towers and MODIS vegetation indices, *J. Arid*  
567 *Environ.*, 70(3), 443–462, doi:10.1016/j.jaridenv.2006.12.026, 2007.

568 Nagler, P. L., Scott, R. L., Westenburg, C., Cleverly, J. R., Glenn, E. P. and Huete, A. R.:  
569 Evapotranspiration on western U.S. rivers estimated using the Enhanced Vegetation Index  
570 from MODIS and data from eddy covariance and Bowen ratio flux towers, *Remote Sens.*  
571 *Environ.*, 97(3), 337–351, doi:10.1016/j.rse.2005.05.011, 2005a.

572 Nagler, P., Glenn, E., Nguyen, U., Scott, R. and Doody, T.: Estimating Riparian and  
573 Agricultural Actual Evapotranspiration by Reference Evapotranspiration and MODIS  
574 Enhanced Vegetation Index, *Remote Sensing*, 5(8), 3849–3871, doi:10.3390/rs5083849,  
575 2013.

576 Nagler, P.: Leaf area index and normalized difference vegetation index as predictors of  
577 canopy characteristics and light interception by riparian species on the Lower Colorado  
578 River, *Agric. For. Meteorol.*, 125(1-2), 1–17, doi:10.1016/j.agrformet.2004.03.008, 2004.

579 Oliveira, P. T. S., Nearing, M. A., Moran, M. S., Goodrich, D. C., Wendland, E., and Gupta,  
580 H. V.: Trends in water balance components across the Brazilian Cerrado, *Water Resour.*  
581 *Res.*, 50, 7100–7114, doi:10.1002/2013WR015202, 2014.

582 Oliveira, P. T. S., Wendland, E. and Nearing, M. A.: Rainfall erosivity in Brazil: A review,  
583 *Catena*, 100, 139–147, doi:10.1016/j.catena.2012.08.006, 2013.

584 Oliveira, R. S., Bezerra, L., Davidson, E. A., Pinto, F., Klink, C. A., Nepstad, D. C. and  
585 Moreira, A.: Deep root function in soil water dynamics in cerrado savannas of central  
586 Brazil, *Funct. Ecol.*, 19(4), 574–581, doi:10.1111/j.1365-2435.2005.01003.x, 2005.

587 Reys, P. A. N.: Estrutura e fenologia da vegetação de borda e interior em um fragmento de  
588 cerrado sensu stricto no sudeste do Brasil (Itirapina, São Paulo), Ph.D. Thesis,  
589 Universidade Estadual Paulista, Rio Claro, SP. Brazil, 2008.

590 Rodrigues, D.B.B., Gupta, H.V., Serrat-Capdevila, A., Oliveira, P.T.S, Mario Mendiondo, E.,  
591 Maddock, T. and Mahmoud, M.: Contrasting American and Brazilian Systems for Water  
592 Allocation and Transfers, *J. Water Res. Pl-Asce*, 04014087,  
593 doi:10.1061/(ASCE)WR.1943-5452.0000483, 2014.

594 Ruhoff, A. L., Paz, A. R., Aragao, L. E. O. C., Mu, Q., Malhi, Y., Collischonn, W., Rocha, H.  
595 R. and Running, S. W.: Assessment of the MODIS global evapotranspiration algorithm  
596 using eddy covariance measurements and hydrological modelling in the Rio Grande basin,  
597 *Hydrolog. Sci. J.*, 58(8), 1658–1676, doi:10.1080/02626667.2013.837578, 2013.

598 Santos, A. J. B., Silva, G. T. D. A., Miranda, H. S., Miranda, A. C. and Lloyd, J.: Effects of  
599 fire on surface carbon, energy and water vapour fluxes over campo sujo savanna in central  
600 Brazil, *Funct. Ecol.*, 17(6), 711–719, doi:10.1111/j.1365-2435.2003.00790.x, 2003.

601 Scanlon, B. R., Reedy, R. C., Stonestrom, D. A., Prudic, D. E. and Dennehy, K. F.: Impact of  
602 land use and land cover change on groundwater recharge and quality in the southwestern  
603 US, *Global Change Biol.*, 11(10), 1577–1593, doi:10.1111/j.1365-2486.2005.01026.x,  
604 2005.

605 Scott, R. L., Cable, W. L., Huxman, T. E., Nagler, P. L., Hernandez, M. and Goodrich, D. C.:  
606 Multiyear riparian evapotranspiration and groundwater use for a semiarid watershed, *J.*  
607 *Arid Environ.*, 72(7), 1232–1246, doi:10.1016/j.jaridenv.2008.01.001, 2008.

608 Soares-Filho, B., Rajao, R., Macedo, M., Carneiro, A., Costa, W., Coe, M., Rodrigues, H. and  
609 Alencar, A.: Cracking Brazil's Forest Code, *Science*, 344(6182), 363–364,  
610 doi:10.1126/science.1246663, 2014.

611 Spracklen, D. V., Arnold, S. R. and Taylor, C. M.: Observations of increased tropical rainfall  
612 preceded by air passage over forests, *Nature*, 489(7415), 282–285,  
613 doi:10.1038/nature11390, 2012.

614 Villalobos-Vega, R., Salazar, A., Miralles-Wilhelm, F., Haridasan, M., Franco, A. C., and  
615 Goldstein, G.: Do groundwater dynamics drive spatial patterns of tree density and diversity  
616 in Neotropical savannas?, *J. Veg. Sci.*, 25, 1465–1473, doi:10.1111/jvs.12194, 2014.

617 Vourlitis, G. L., Filho, N. P., Hayashi, M. M. S., Nogueira, J. S., Caseiro, F. T., and Campelo  
618 Jr., J. H.: Seasonal variations in the evapotranspiration of a transitional tropical forest of  
619 Mato Grosso, Brazil, *Water Resour. Res.*, 38, 1–11, doi:10.1029/2000WR000122, 2002.

620 Wang, K., Wang, P., Li, Z., Cribb, M., and Sparrow, M.: A simple method to estimate actual  
621 evapotranspiration from a combination of net radiation, vegetation index, and temperature,  
622 *J. Geophys. Res.*, 112, 1–14, doi:10.1029/2006JD008351, 2007.

623 Wendland, E., Barreto, C. and Gomes, L. H.: Water balance in the Guarani Aquifer outcrop  
624 zone based on hydrogeologic monitoring, *J. Hydrol.*, 342(3–4), 261–269,  
625 doi:10.1016/j.jhydrol.2007.05.033, 2007.

626 Wohl, E., Barros, A., Brunzell, N., Chappell, N. A., Coe, M., Giambelluca, T., Goldsmith, S.,  
627 Harmon, R., Hendrickx, J. M. H., Juvik, J., McDonnell, J., and Ogden, F.: The hydrology  
628 of the humid tropics, *Nat. Clim. Change*, 655–662, doi:10.1038/nclimate1556, 2012.

629 Youlton, C.: Quantificação experimental da alteração no balanço hídrico e erosão em um  
630 neossolo quartzarênico devido à substituição de pastagem por cana-de-açúcar, Ph.D.  
631 Thesis, Universidade de São Paulo, São Carlos, SP, Brazil, 2013.

632 Table 1. Summary of characteristics of the studied areas.

Description	PDG	IAB
Köppen climate classification system	Cwa humid subtropical	Cwa humid subtropical
Average annual precipitation (mm) and temperature (°C)	1478 and 21.1	1506 and 20.8
Soil texture	sandy texture	sandy texture
Vegetation physiognomy	"cerrado sensu stricto denso"	"cerrado sensu stricto denso"
Absolute density of trees	15,278 individuals per hectare*	13,976 individuals per hectare**

633 \* Reys 2008 and \*\* Fidelis and Godoy, 2003.

634

635 Table 2. Data collected at the IAB site.

<b>Variable description</b>	<b>Sensor</b>	<b>Height or depth (m)</b>
Temperature and relative humidity	Psychrometer HC2S3	9
Wind speed and direction anemometer	Anemometer RM Young 05103-5	10
Net radiation	NR-LITE2	10
Global solar radiation	LiCor 200X	10
Precipitation	Texas TB4	10
Atmospheric pressure	Barometer Vaisala CS106	2
Soil moisture	EnviroScan SENTEK	0.10, 0.50, 0.70, 1.00, 1.50

636

637 Table 3. Model calibration and validation results reported as the coefficient of determination ( $R^2$ ), standard  
638 deviation of differences (SD), and root mean square errors (RMSE) for 16-day averages

<b>Time series</b>	<b><math>R^2</math></b>	<b>SD (mm day<sup>-1</sup>)</b>	<b>RMSE (%)</b>
Calibration, 2001-2002	0.71	0.50	20.92
Validation, 2003	0.83	0.33	15.69
Full time series, 2001-2003	0.73	0.45	19.53

639



640 Table 4. Previous studies of throughfall (TF) and stemflow (SF) in the Brazilian Cerrado. Percentages denote  
 641 percent of total rainfall.

<b>Location</b>	<b>Land cover</b>	<b>TF (%)</b>	<b>SF (%)</b>	<b>Source</b>
Agudos, São Paulo Satate	"cerradão"	72.7	-	Lima and Nicolielo, 1983
Uberlândia, São Paulo Satate	"cerrado sensu stricto"	89.0	< 1	Lilienfein and Wilcke, 2004
Assis, São Paulo Satate	"cerrado sensu stricto"	95.0	0.7	Honda, 2013
Assis, São Paulo Satate	"cerrado sensu stricto denso"	89.0	1.5	Honda, 2013
Assis, São Paulo Satate	"cerradão"	80.0	2.4	Honda, 2013
Itirapina, São Paulo Satate	"cerrado sensu stricto denso"	81.2	1.1	Present study

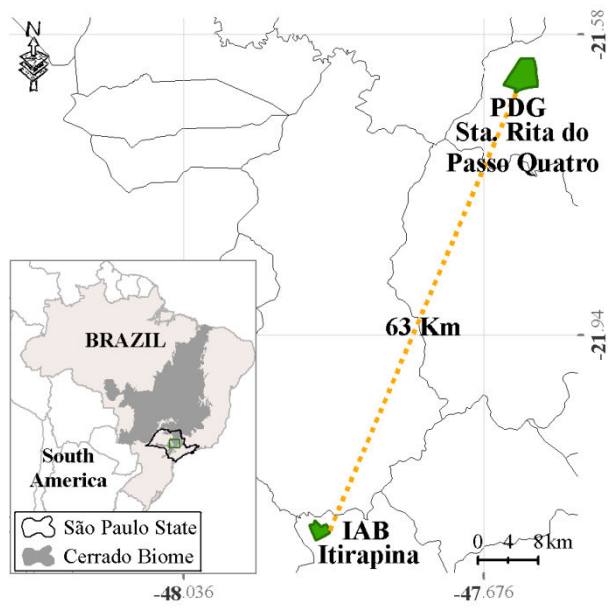
642

643 Table 5. Average evapotranspiration for PDG and IAB sites.

<b>Evapotranspiration (ET)</b>	<b>PDG</b>	<b>IAB</b>
ET full period (mm d <sup>-1</sup> )	2.31 ± 0.87	2.30 ± 0.67
ET wet season (mm d <sup>-1</sup> )	2.81 ± 0.57	2.60 ± 0.38
ET dry season (mm d <sup>-1</sup> )	1.70 ± 0.70	1.91 ± 0.60
Annual ET (mm yr <sup>-1</sup> )	822	823

644

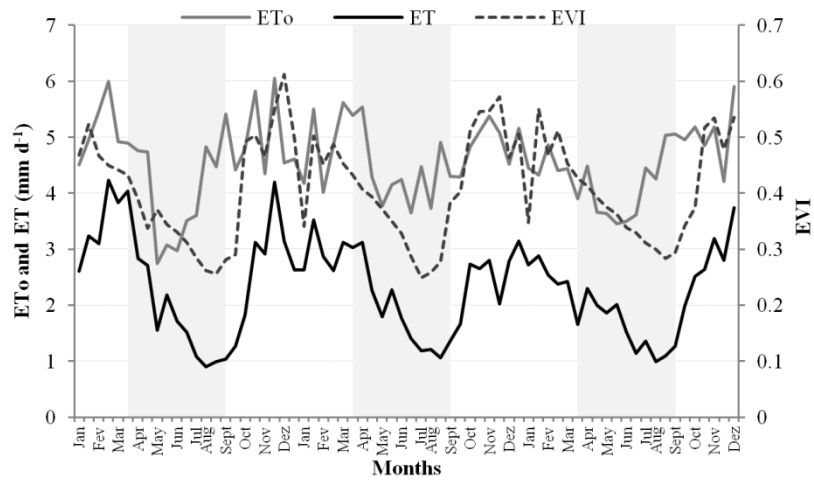
645



646

647 **Figure 1.** Location of study areas.

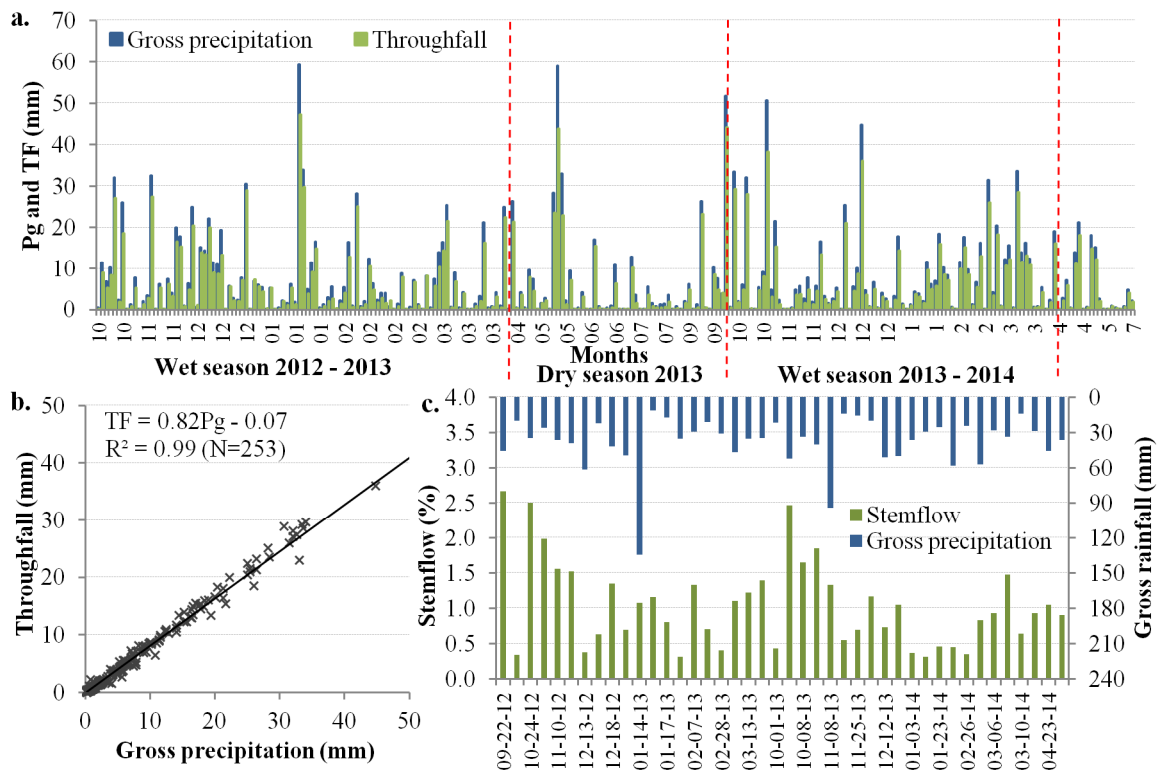
648



649

650 **Figure 2.** Seasonality of enhanced vegetation index (EVI), reference evapotranspiration  
 651 (ETo) and observed actual evapotranspiration (ET) data from 2001 through 2003 at the PDG  
 652 site. The grey shaded bars show the dry seasons.

653

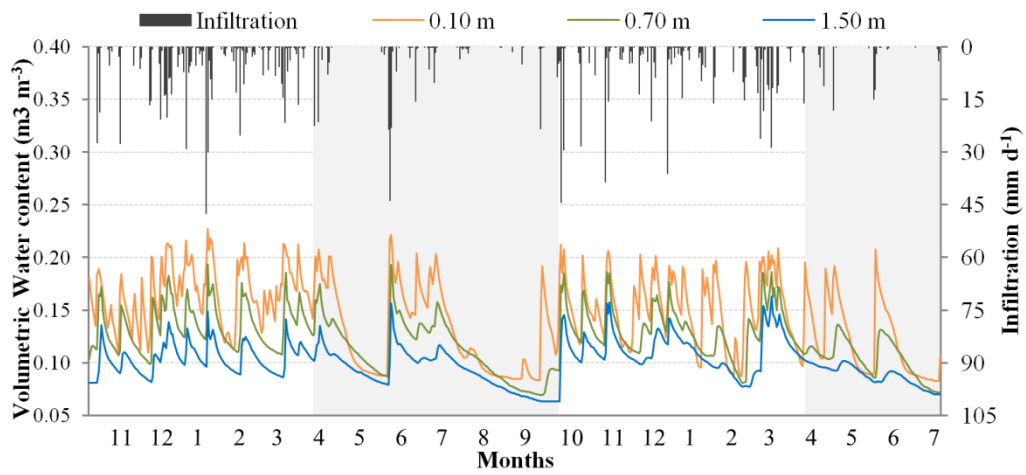


654

655 **Figure 3. a.** Gross precipitation and throughfall for each rain event measured from October,  
 656 2012 through July, 2014. Dotted lines in red show the beginning and the end of dry seasons  
 657 (April through September). **b.** Scatter plot of throughfall against gross precipitation. **c.** Gross  
 658 precipitation and stemflow measured from September 2012 through May 2014.

659

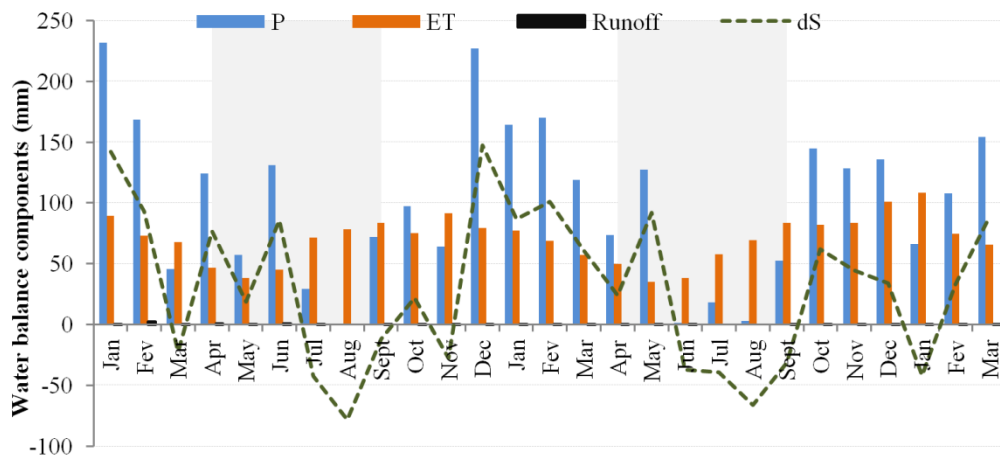
660



661

662 **Figure 4.** Estimated infiltration and volumetric water content measured at the depth of 0.10  
663 m, 0.70 m, and 1.50 m. Data were collected from October 2012 through July 2014. The grey  
664 shaded bars show the dry seasons.

665



666

667 **Figure 5.** Water balance components at monthly scale from January 2012 through March  
 668 2014. The grey shaded bars show the dry seasons. *P* is precipitation, *ET* is evapotranspiration,  
 669 and *dS* is soil water storage.